IOPscience iopscience.iop.org

Home Search Collections Journals About Contact us My IOPscience

Ab initio calculation of electronic properties of $Ga_{1-x}Al_xN$ alloys

This article has been downloaded from IOPscience. Please scroll down to see the full text article.

1997 J. Phys.: Condens. Matter 9 1763

(http://iopscience.iop.org/0953-8984/9/8/008)

View the table of contents for this issue, or go to the journal homepage for more

Download details:
IP Address: 171.66.16.151
The article was downloaded on 12/05/2010 at 23:05

Please note that terms and conditions apply.

J. Phys.: Condens. Matter **9** (1997) 1763–1775. Printed in the UK PII: S0953-8984(97)76620-7

Ab initio calculation of electronic properties of $Ga_{1-x}Al_xN$ alloys

Bal K Agrawal, Savitri Agrawal, P S Yadav and Sudhir Kumar

Physics Department, Allahabad University, Allahabad 211002, India

Received 24 July 1996, in final form 13 November 1996

Abstract. The electronic properties of the wide-band-gap semiconducting ordered $Ga_{1-x}Al_xN$ alloys (for $x = 0.0$, 0.25, 0.50, 0.75 and 1.0) and the random alloys have been investigated by using a full-potential self-consistent linear muffin tin orbital (LMTO) method. The calculated direct band gap for random distribution of cation nearest-neighbour tetrahedral clusters in the $Ga_{1-x}Al_xN$ alloys for any arbitrary concentration x is seen to show a quite linear variation in agreement with the experiment. On the other hand, the indirect band gap remains invariant. We observe a direct to indirect band gap crossover at $x = 0.59$. The band gap bowing is seen to be very small.

1. Introduction

There has been tremendous interest in the development of optoelectronic devices, especially for obtaining light emitting diodes and laser emitting devices in the ultraviolet region (Lei and Moustakas 1992, Van der Walle 1993, Wettling and Windschif 1984, Xia *et al* 1993). This has led to a search for wide-band-gap semiconductors possessing band gaps of more than 2.0 eV. One type of candidate is GaN, AlN, and their alloys, opening a possibility of varying the band gap from 3.4 eV in GaN to 6.2 eV in AlN. The emitted short-wavelength electromagnetic radiation will lie up to the ultraviolet region.

The development of the epitaxial growth technique has made possible the preparation of semiconductor grade films of $Ga_{1-x}Al_xN$ alloys (x is the fractional concentration of Al atoms). Intrinsic carrier concentrations in the range 10^{16}–10^{17} cm^{-3} and mobilities up to 600 cm^2 V^{-1} s^{-1} have been measured (Amano *et al* 1989). Controlled p-type (with Mg) and n-type (with Si) doping has been achieved (Akasaki and Amano 1992, Molnar and Moustakas 1993, Nakamura *et al* 1991). Akasaki and Amano (1992) have demonstrated the fabrication of the light emitting diodes in the ultraviolet region from $Ga_{1-x}Al_xN$/GaN heterostructures and also stimulated emission.

In their natural form, both GaN and AlN possess the hexagonal wurtzite structure. However, it has been possible to have a stabilized zinc-blende structure of GaN on GaAs(001) substrates (Martin *et al* 1991, Mizuta *et al* 1986, Ueno *et al* 1994, Miwa and Fukumotoa 1993, Strike *et al* 1991) and also on cubic SiC(001) substrates (Paisley *et al* 1989, 1992, Gorczyka and Christensen 1991, Perlin *et al* 1992a, b, Schrwin and Drummond 1991). Also, there is evidence of the zinc-blende AlN in the form of precipitates (Lei *et al* 1992). It has been seen that the energy difference between the wurtzite and zinc-blende structures of GaN and AlN per unit cell is quite small, of the order of 20–30 meV for GaN (Muñoz and Kunc 1991, Yeh *et al* 1992) and 36 meV for AlN (Lambrecht and Segall 1992).

0953-8984/97/081763+13$19.50 © 1997 IOP Publishing Ltd

On the theoretical side, only a very few first-principles calculations have been performed to elucidate the physical properties of $Ga_{1-x}Al_xN$ alloys. Albanesi *et al* (1993) have performed an LMTO calculation in the atomic sphere approximation (ASA) and have shown a weak bowing in the variation of the energy gap.

Usually in the application of the standard LMTO method, an atomic sphere approximation (ASA) is used to make it efficient. However, this LMTO–ASA method suffers from several disadvantages. (i) It neglects the symmetry breaking terms by discarding the nonspherical parts of the electron density. (ii) The method discards the interstitial region by replacing the muffin tin spheres by space filling Wigner spheres. (iii) It uses spherical Hankel functions with vanishing kinetic energy only.

The present LMTO method (Methfessel 1988) goes beyond the LMTO method usually employed in the ASA.

2. Theory

2.1. The LMTO method

It has been noted that quite reliable results can be attained by employing an LMTO basis set if all the potential terms are determined accurately. For this, the sizes of the atomic spheres are shrunk so as to make them nonoverlapping. The potential matrix elements are then split into two parts, one contribution from the atomic spheres and the other from the complicated interstitial region. The first part, i.e. the atomic sphere one, is easy to evaluate by expanding it in terms of the usual spherical harmonics. On the other hand, the evaluation of the interstitial contribution is quite difficult and very time consuming if done by standard techniques. Efforts have been made to find an efficient and quick way to determine the interstitial contribution. In the method used in the present work, the interstitial quantities were expanded in terms of the spherical Hankel functions. The three-centre integrals involved were expressed as linear combinations of the two-centre integrals by numerical means. These two-centre integrals, involving Hankel functions, can easily be evaluated analytically. The method is applicable to the periodic as well as the nonperiodic systems which so often need to be treated especially when impurities, defects and lattice distortions or atomic relaxations occur.

2.2. Statistical properties of disordered alloys

The statistical mechanical properties of the disordered alloys can be obtained by using the cluster expansion method (Sanchez and de Fontaine 1981, Sanchez *et al* 1984, Srivastava *et al* 1985) and the idea of Connolly and Williams (1983) who suggested that the coefficients of the cluster expansion may be derived by a first-principles calculations of a set of ordered compounds. The method which was primarily used for the binary alloys may easily be applied to the ternary alloys if one assumes that the disorder occurs only on one type of site, say cation, as is the case for the $Ga_{1-x}Al_xN$ alloys (x denotes the fractional concentration). The problem further simplifies if one truncates the cluster expansion at the level of the nearest-neighbour tetrahedron interactions. One may consider the five basic types of cation nearest-neighbour tetrahedron $A_{4-n}B_n$ with the values of the integer $n = 0$–4. Let $P_n(x)$ be the probability of the occurrence of the cation tetrahedrons $A_{4-n}B_n$ in the disordered alloy of concentration x. Then, a property F may be expanded as

$$F(x) = \sum_n P_n(x) F_n \tag{1}$$

where F_n is the property for the cation tetrahedron $A_{4-n}B_n$.

In the cluster expansion method, one has to determine the probability of each cluster $P_n(x, T)$ at a given temperature T by minimizing the free energy with respect to $P_n(x, T)$. We assume (similar to others, e.g. Srivastava *et al* 1985, Albanesi *et al* 1993) a temperature independent random distribution function,

$$P_n(x) = \binom{4}{n} x^n (1-x)^{4-n}. \tag{2}$$

Obviously, this is a first approximation but it may be valid for the case of frozen-in disorder of the gas or liquid phase from which the solid solutions are quenched.

In the present study, we have not relaxed the bond lengths as has been studied by Srivastava *et al*, who have pointed out that positive optical bowing may result by local bond relaxation effects.

In the present investigations, the full-potential LMTO method has been used to study the electronic properties of GaN, AlN and their ordered and random alloys $Ga_{1-x}Al_xN$. The calculated results of the electronic structure, total density of states and the electronic charge densities for the GaN, AlN and $Ga_{1-x}Al_xN$ systems using an eight-atom supercell are presented in section 3. Section 4 includes the main conclusions.

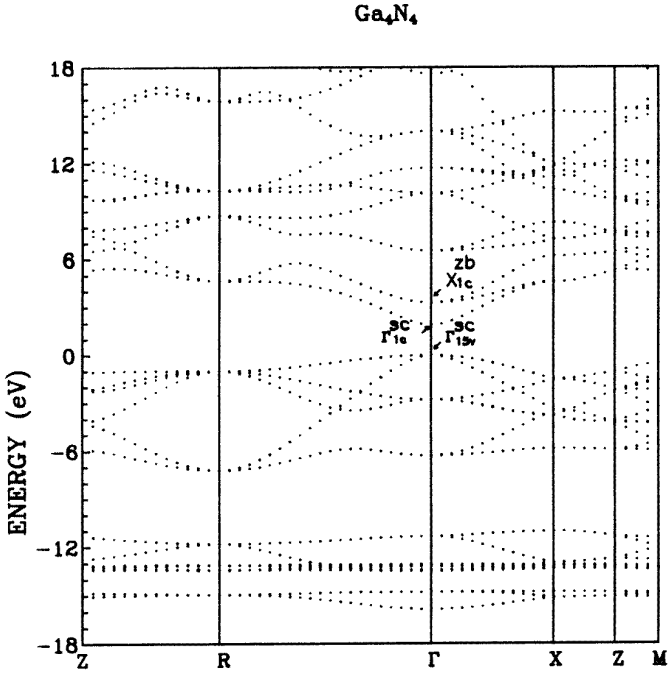

Figure 1. The dispersion curves for a Ga_4N_4 supercell containing an eight-atom unit cell.

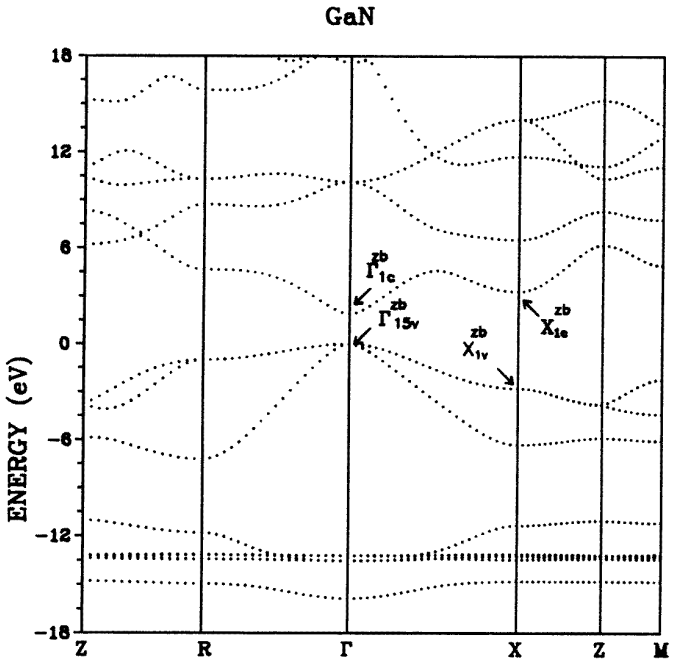

Figure 2. The dispersion curves for GaN containing a two-atom unit cell.

3. Calculation and results

We employ a unit cell containing four molecular units, i.e. $Ga_{4-n}Al_nN_4$ for $n = 0$–4. In order to reproduce the usual zinc-blende structure for this quadrupole unit cell, one has to use a different lattice, namely the simple cubic (sc) one with the translation vector of length a. As has also been pointed out by Srivastava *et al*, various crystal structure choices for $n = 1, 2, 3$ are possible.

In the present method (Methfessel 1988, Agrawal *et al* 1994a, Agrawal and Agrawal 1994a, b, 1995), we expand the multiple products of the LMTO envelopes required for the charge density and the potential in terms of the Hankel functions with the spherical harmonic components $l \leqslant 4$ and of the kinetic energies -0.01, -1.0, and -2.3 Ryd with the two different types of decay specified by $\lambda^2 = -1$ and 3 Ryd. The supercell contains eight real and eight empty spheres. All the calculations have been performed considering the scalar relativistic effects. The Hedin–Lundquist (1971) parametrization of the exchange–correlation potential was employed in the calculations. The core electrons are allowed to relax and the core electron charge density is recalculated in each iteration of the self-consistent calculation. The value of the calculated fundamental energy gap in the local density approximation is usually seen to be smaller than the experimental value. This is understood to originate from the fact that the eigenvalues of the Kohn–Sham equation (Perdew and Levy 1983, Sham and Schluter 1983) are not excitation energies of the systems. Good estimates of the energy gap may be obtained by solving the quasi-particle equations (Goodby *et al* 1986) when the exchange and correlation effects are described by the self-energy. This self-energy is a nonlocal energy-dependent effective potential. However, this

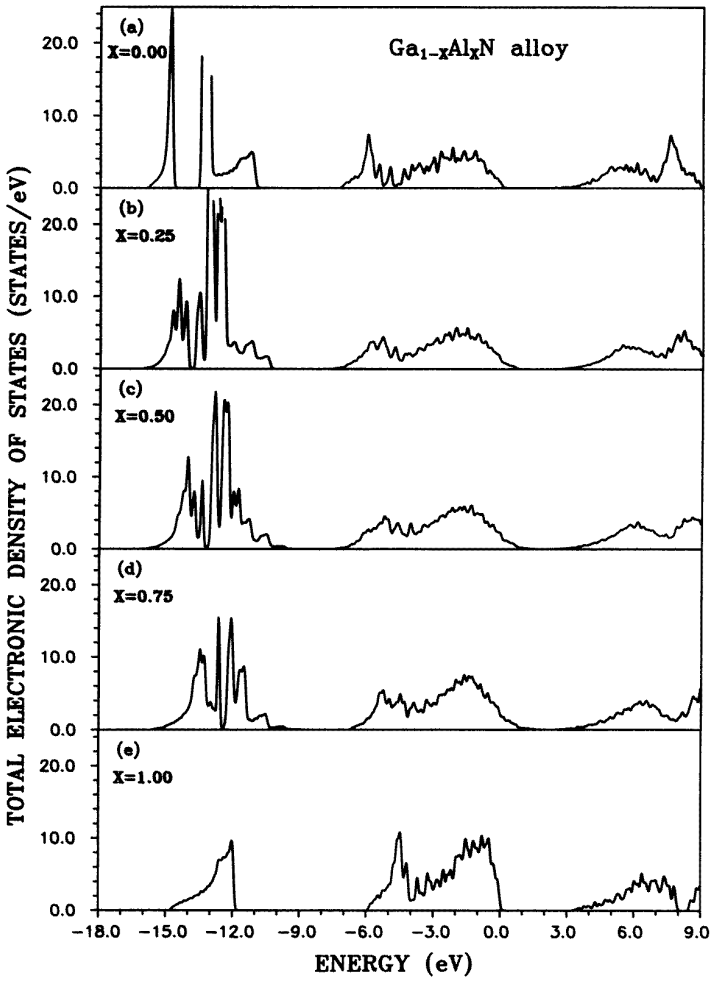

Figure 3. The total electronic density of states for random $Ga_{1-x}Al_xN$ alloys for (a) $x = 0.0$, (b) $x = 0.25$, (c) $x = 0.50$, (d) $x = 0.75$ and (e) $x = 1.0$.

is beyond the scope of the present work.

As noted above, the lattice is sc for the quadrupole unit cell used, which, in turn, leads to an sc Brillouin zone. Also, the electronic structure corresponding to the quadrupole unit cell will exhibit folding of the dispersion curves which will be discussed in detail a little later.

The radii of the nonoverlapping spheres around each atom were varied to see the variation in the values of the lattice parameters. The variation was made from that of equal radii for both cation and anion to unequal radii proportional to the atomic radii of the atoms. The values of determined equilibrium lattice parameters change within 1–2%.

The calculated lattice parameters for the minimum lattice energy volumes are compared with the other calculations and the available experimental data for the ordered $Ga_{1-x}Al_xN$ structures in table 1. The variation in the lattice parameter is seen to be linear. Our values

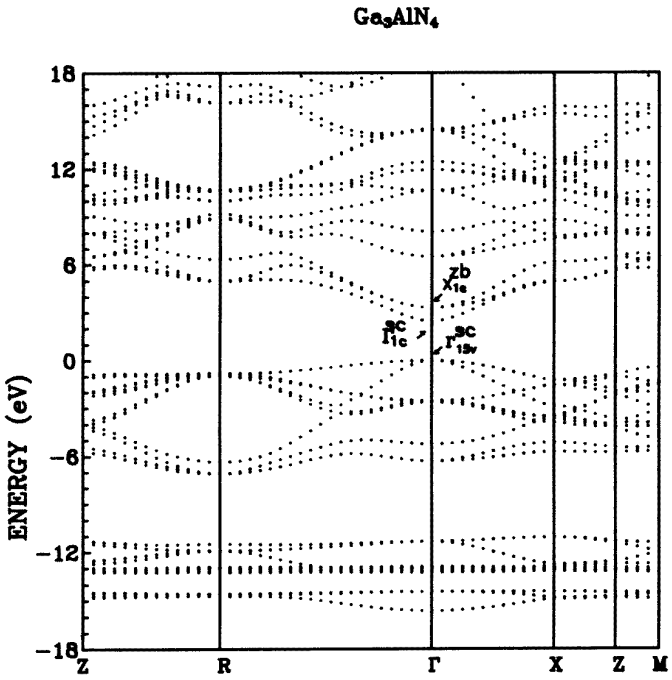

Figure 4. The dispersion curves for the ordered Ga_3AlN_4 structure.

are quite similar to those obtained by Albanesi *et al* (1993) and are in excellent agreement with the experiment for the end alloys. Our values are slightly on the higher side. We now discuss each alloy separately.

Table 1. Calculated lattice constants (in ångströms) for the ordered $Ga_{1-x}Al_xN$ structures.

Systems	Present work	Other calculation	Experiment
GaN	4.510 ± 0.010	4.48[a], 4.42[b],4.30[c]	4.50[d]
$Ga_{0.75}Al_{0.25}N$	4.485 ± 0.005	4.46[a]	
$Ga_{0.50}Al_{0.50}N$	4.450 ± 0.010	4.43[a]	
$Ga_{0.25}Al_{0.75}N$	4.415 ± 0.015	4.39[a]	
AlN	4.370 ± 0.020	4.35[a,b]	4.37[d]

[a] LMTO–ASA (Albanesi *et al* 1993).
[b] Pseudo-potential (Rubio *et al* 1993, 1995).
[c] Pseudo-potential (Jenkins *et al* 1994).
[d] Wyckoff (1964).

3.1. GaN

The radius of the non-overlapping spheres drawn around each real and empty atom was chosen as 1.815 au. Ga (4s, 4p, 3d) and N (2s, 2p) states are considered as the valence states. The point group symmetry at each site is T_d. The calculations were performed for

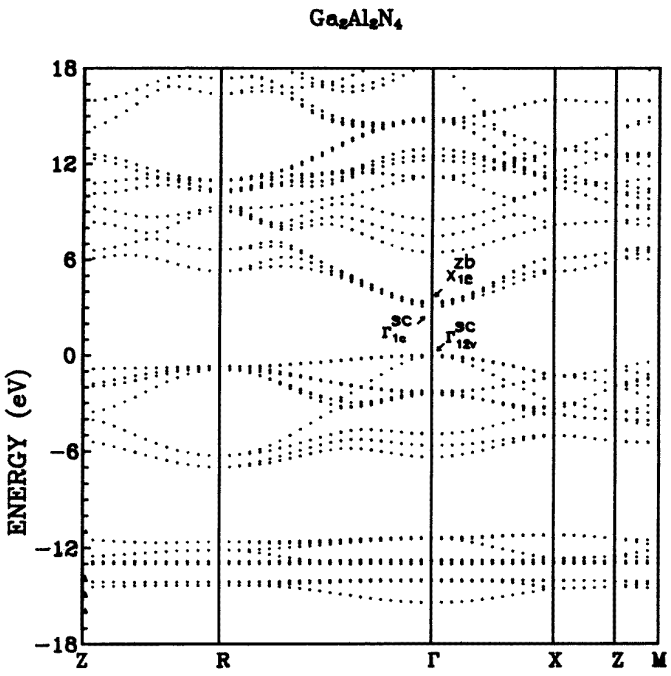

Figure 5. The dispersion curves for the ordered $Ga_2Al_2N_4$ structure.

28 selected $\boldsymbol{k}$-points in the irreducible part of the Brillouin zone to achieve self-consistency in the charge density.

The electronic dispersion curves for GaN are presented in figure 1. In order to facilitate comparison, we present here the electronic structure for the simplest two-atom unit cell of GaN having a zinc-blende structure in figure 2. One observes a direct band gap. The comparatively flat 3d states of Ga appear just near the bottom of the valence band and they hybridize strongly with the 2s states of N.

The symmetry points for the sc Brillouin zone for the super unit cell as shown in figure 1 are $\Gamma(0, 0, 0)$, $X(1, 0, 0)$, $M(1, 1, 0)$, $R(1, 1, 1)$ and $Z(1, 0.5, 0)$. The nomenclature of symmetry points except the Γ and X points is different from those of the symmetry points of the bcc Brillouin zone of the zinc-blende structure. As pointed out earlier, the electronic structure of the eight-atom unit cell shows zone folding. Thus, at the Γ-point, the state appearing at the conduction band minimum of the sc Brillouin zone is related to the lowest conduction state at the X point of the zinc-blende Brillouin zone. At the Γ-point, along with the triplet value valence states Γ_{15v}^{sc} at the top of the valence band and the singlet conduction Γ_{1c}^{sc} state lying at the bottom of the conduction band, there is an extra state X_{1c}^{zb} just above the Γ_{1c}^{sc} state, which corresponds to the X point of the zinc-blende structure. The direct band gap of 1.9 eV appearing in the two-atom unit cell remains a direct one in the Ga_4N_4 unit cell. However, the same is not true for the systems showing indirect band gaps for large concentrations of Al atoms as seen later.

The electron density of states has been obtained by employing 110 selected $\boldsymbol{k}$ points in the irreducible part of the Brillouin zone with a Gaussian broadening of 0.005 Ryd. The

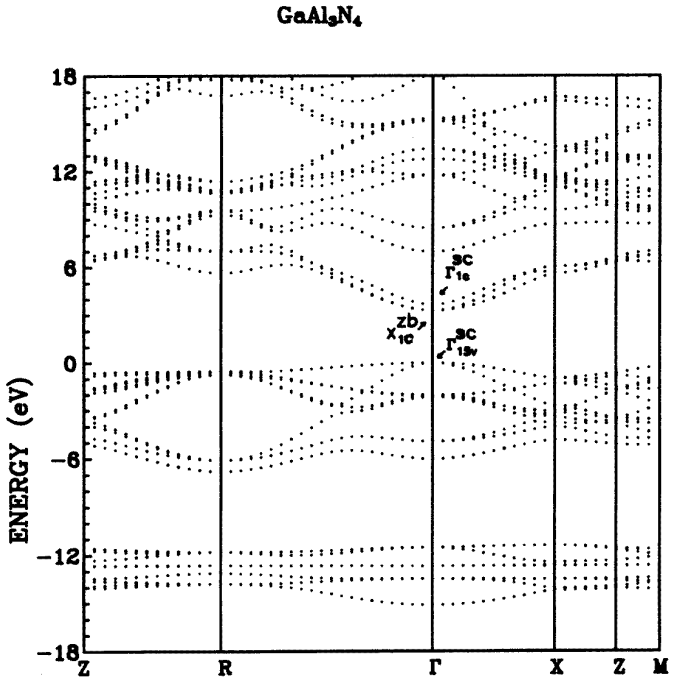

Figure 6. The dispersion curves for the ordered $GaAl_3N_4$ structure.

result for the total density of states for the Ga_4N_4 ordered structure is shown in figure 3(a).

The bottom of the valence band extends up to −16.0 eV and is comprised of mainly the Ga 3d states slightly mixed with the N 2s sates. The main peaks in this region appear near −14.8, −13.3, and −11.3 eV. The states near the top of the valence band arise mainly from the hybridized N 2p and Ga 4p-like orbitals and they extend up to 7.5 eV towards the low-energy side.

The density functional theory–local density approximation gap is always smaller than the experimental value (3.55 eV in wurtzite GaN), and reported values for cubic GaN range from 3.25 to 3.5 eV (Davis 1991, Powell *et al* 1990).

3.2. Ordered $Ga_{1-x}Al_xN$ alloys

For the $Ga_{0.75}Al_{0.25}N$ ordered alloy ($x = 0.25$), the calculations were performed for 58 $\boldsymbol{k}$ points in the irreducible part of the Brillouin zone to achieve self-consistency in the charge density. For Al, the valence states are Al(3s, 3p, 3d). The calculated dispersion curves are presented in figure 4. The point group symmetry at the N atom is C_{3v}. The dispersion curves are approximately similar to those of GaN as shown in figure 2 except the splitting of states because of the lower point group symmetry. The fundamental gap is direct and has a value of 2.46 eV. The other results are similar to those for Ga_4N_4.

The ordered structure $Ga_2Al_2N_4$ has a C_{2v} point group symmetry at N and the self-consistent calculation has been performed for 98 selected $\boldsymbol{k}$ points. The dispersion curves for the $Ga_{0.50}Al_{0.50}N$ alloy are presented in figure 5. They are very similar to those of the

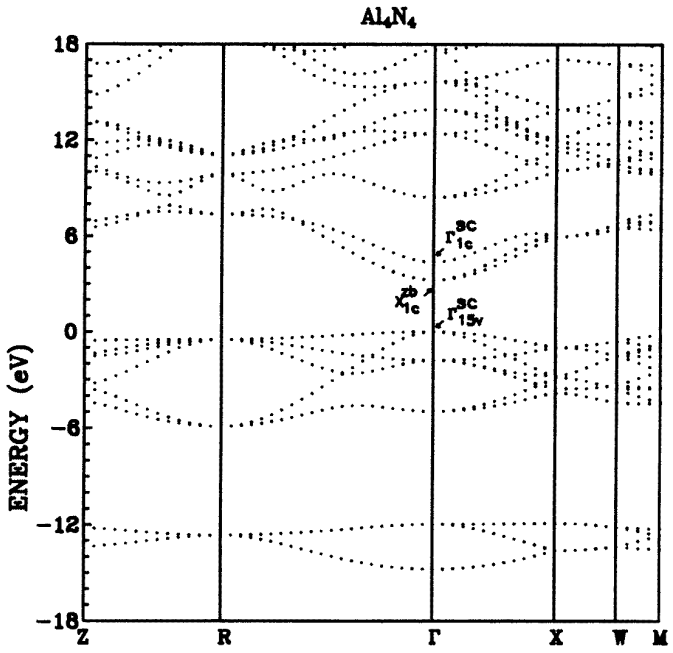

Figure 7. The dispersion curves for an Al_4N_4 super cell containing an eight-atom unit cell.

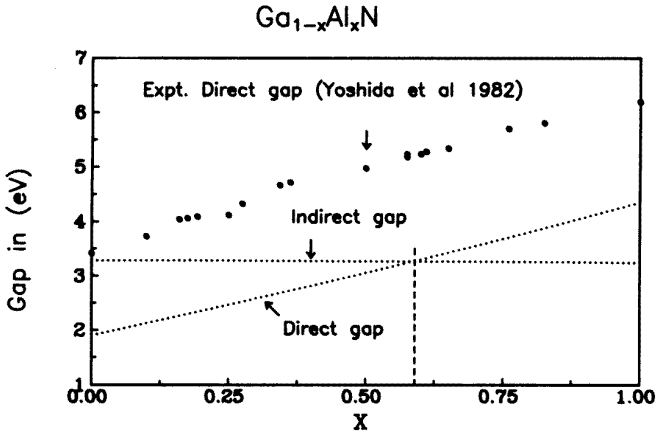

Figure 8. The variation of band gap (eV) with the concentration x in the random $Ga_{1-x}Al_xN$ alloys.

$Ga_{0.75}Al_{0.25}N$ alloy except that the number of split bands increases further because of a lower point group symmetry. Here again, the order of the states at the Γ point is similar to those of the Ga_4N_4 ordered structure.

The dispersion curves for the ordered $Ga_{0.25}Al_{0.75}N$ alloy are shown in figure 6. The point group symmetry at the N atom is again C_{3v} and the self-consistent calculations have

been performed for 58 selected $\boldsymbol{k}$ points. Here, one finds that at the Γ point the lowest conduction state corresponds to the X_{1c}^{zb} symmetry of the Brillouin zone of the zinc-blende structure. The conduction state Γ_{1c}^{sc} of the super unit cell appears above the X_{1c}^{zb} state. This result is in contrast to those of the other structures containing smaller concentrations of Al atoms. The gap which appears to be direct here is, in fact, indirect and one may call it a pseudo-direct band gap. The indirect band gap has a magnitude of 3.28 eV as compared to the direct band gap of 3.66 eV. This reverse in the order of Γ_{1c}^{zb} and X_{1c}^{zb} in AlN originates from the fact that the Γ_{1c}^{zb} state is sensitive to the potential around the cation nucleus. For cation Al, the atomic number Z is smaller than that of Ga and, therefore, the potential is weaker and this leads the Γ_{1c}^{zb} state to appear above the X_{1c}^{zb} state. On the other hand, the X_{1c}^{zb} state is an antibonding mixed state of the s state of the anion and the p state of the cation. As the p-state wavefunctions vanish at the nucleus, they are less sensitive to Z. This results in the similarity of the X_{1c}^{zb} state in GaN and AlN.

3.3. Al_4N_4

The radius of the muffin tin sphere for each atom is 1.76 au. The computed dispersion curves along symmetry axes are shown in figure 7.

The order of states at the Γ point for Al_4N_4 in the neighbourhood of the fundamental energy gap is similar to that of the $GaAl_3N_4$ ordered structure, i.e. they are in the sequence Γ_{15v}^{sc}, X_{1c}^{zb}, and Γ_{1c}^{sc} towards the high-energy side. The band is indirect as is also seen in the two-atom unit cell of the zinc-blende structure of AlN. The density of states has been computed again for a mesh of 110 special $\boldsymbol{k}$ points in the irreducible part of the Brillouin zone with a Gaussian broadening of 0.005 Ryd. The total density of states is depicted in figure 3(e). In contrast to GaN, the states in the neighbourhood of the top of the valence band now originate from the hybridized Al(3p, 3d) and N(2p) states and their contributions are comparable. The ionic gap is now much larger. The states near the bottom of the valence band are comprised of the hybridized Al(3s, 3p, 3d) and N(2s) states. The indirect band gap is 3.23 eV in contrast to the direct one, which is 4.35 eV.

3.4. Random $Ga_{1-x}Al_xN$ alloys ($x = 0.25, 0.50, 0.75$)

3.4.1. Electronic density of states. For the $Ga_{1-x}Al_xN$ random alloy ($x = 0.25$), the total electronic density of states was obtained for 290 selected $\boldsymbol{k}$ points of the irreducible part of the Brillouin zone and is presented in figure 3(b). The main peaks appear near -14.5, -13.0, -11.2, -5.8, and -2.1 eV.

For the $x = 0.50$ random alloy, the total electronic density of states has been computed for 455 selected $\boldsymbol{k}$ points and the result is shown in figure 3(c). The low-lying peaks appear near -14.1, -12.8, -11.8, -5.1, and -1.4 eV. The major peaks are slightly shifted towards the higher-energy side with increasing x.

For the $x = 0.75$ random alloy, the total electronic density of states has been determined for 290 selected $\boldsymbol{k}$ points in the irreducible part of the Brillouin zone and is shown in figure 3(d). The main peaks in the valence band region are near -13.5, -12.6, -11.5, -5.2, and -1.6 eV. The density is comparatively high near the top of the valence band. We are not aware of any experimental data for the random alloys for comparison.

3.4.2. The energy gap. Equations (1) and (2) are utilized to determine the variation of the direct and indirect energy gaps for the various concentrations of the constituent atoms in the random $Ga_{1-x}Al_xN$ alloys. The calculated values are compared with the experimental points

Table 2. The energy gap (eV) in the zinc-blende structure for the ordered $Ga_{1-x}Al_xN$ structures.

Systems	Transition	Present work	Other calculations	Experiment
GaN	Γ_{15v}–Γ_{1c}	1.9[d]	2.23[a], 2.0[b], 1.97[c], 2.01[e], 2.1[f], 2.08[g], 2.32[h]	3.52[j], 3.2[k], 3.4[l], 3.3[m]
	Γ_{15v}–X_{1c}	3.28[i]	3.36[a], 3.16[c], 3.2[f]	
$Ga_{0.75}Al_{0.25}N$	Γ_{15v}–Γ_{1c}	2.46[d]	2.51[c]	4.05[l]
	Γ_{15v}–X_{1c}	3.29[i]	3.35[c]	
$Ga_{0.50}Al_{0.50}N$	Γ_{12v}–Γ_{1c}	3.01[d]	3.06[c]	4.9[l]
	Γ_{12v}–Γ_{12c}	3.24[i]	3.45[c]	
$Ga_{0.25}Al_{0.75}N$	Γ_{15v}–Γ_{1c}	3.66[d]	3.67[c]	5.6[l]
	Γ_{15v}–X_{1c}	3.28[i]	3.22[c]	
AlN	Γ_{15v}–X_{1c}	4.35[d]	4.53[a], 4.25[c], 4.52[e], 4.2[f]	6.1[l], 6.28[n]
	Γ_{15v}–X_{1c}	3.23[i]	3.40[a], 3.16[c], 3.2[f]	

[a] LMTO–ASA (Christensen and Gorczyca 1994).
[b] FP–LMTO (Fiorentini *et al* 1993).
[c] LMTO–ASA (Albanesi *et al* 1993).
[d] Direct gap.
[e] LMTO (Lambrecht and Segall 1994).
[f] Norm conserving pseudopotential (Rubio *et al* 1993).
[g] Norm conserving pseudopotential (Min *et al* 1992).
[h] Pseudopotential (Jenkins *et al* 1994).
[i] Indirect gap.
[j] Cathodoluminescence at 53 K on epitaxial films (Harrison 1985).
[k] Optical absorption (Lei *et al* 1992).
[l] Optical absorption (Yoshida *et al* 1982).
[m] Photoluminescence and cathodoluminescence (Paisley *et al* 1989, 1992).
[n] Optical absorption at 300 K in wurtzite structure (Perry and Rutz 1978).

in figure 8. One observed that the indirect gap shows little variation with the concentration. On the other hand, the direct gap shows a rapid variation, which is very much linear except a quite small bowing in the middle of the concentration range, but this small bowing is opposite to that observed by Yoshida *et al* (1982). It seems that the experimentally observed bowing may not arise from the disorder in the composition of atoms but from other types of disorder such as bond length relaxation as has been seen by Albanesi *et al* (1993).

From table 2, we observe that for the ordered systems $GaAl_3N_4$ and Al_4N_4 the gap is seen to be indirect. A perusal of figure 8 reveals a crossover from direct to indirect gap for the random $Ga_{1-x}Al_xN$ alloys at a concentration of $x = 0.59$ for which the energy gap $E_g = 3.26$ eV. These results are in agreement with those of Albanesi *et al* (1993) who have obtained a crossover at $x = 0.57$ and $E_g = 3.22$ eV.

4. Conclusions

The full-potential LMTO method is capable of predicting quite well the electronic properties of the alloys of the wide-band-gap semiconductors. A nearly linear variation with the concentration x in the ordered and random $Ga_{1-x}Al_xN$ configurations has been observed

in the lattice constant and the direct energy band gap, respectively. On the other hand, the indirect energy band gap remains invariant. By employing a cation nearest-neighbour tetrahedron approximation in the cluster expansion method, we observe a direct to indirect gap crossover at $x = 0.59$. The band gap bowing is seen to be very small.

Acknowledgments

The authors are thankful to the University Grants Commission, New Delhi, and the Department of Science and Technology, New Delhi, for financial assistance.

References

Agrawal B K and Agrawal S 1994a *Physica* C **234** 29
——1994b *Physica* C **233** 8
——1995 *Preprint*
Agrawal B K, Yadav P S and Agrawal S 1994 *Phys. Rev.* B **50** 14 881
Akasaki I and Amano H 1992 *Wide Band Gap Semiconductors (MRS Symp. Proc. 242)* ed T D Moustakas, J I Pankove and Y Hamakawa (Pittsburgh, PA: Materials Research Society) p 383
Albanesi E A, Lambrecht W R L and Segall B 1993 *Phys. Rev.* B **48** 17 841
Amano H, Kito M and Hiramitsu K 1989 *Japan. J. Appl. Phys.* **28** L2112
Christensen N E and Gorczyca I 1994 *Phys. Rev.* B **50** 4402
Connolly J W D and Williams A R 1983 *Phys. Rev.* B **27** 5169
Davis R F 1991 *Proc. IEEE* **79** 702
Fiorentini V, Methfessel M and Scheffler M 1993 *Phys. Rev.* B **47** 13 353
Gerlich D S, del Sole L and Slack G A 1986 *J. Phys. Chem. Solids* **47** 437
Goodby R W, Schulter M and Sham L J 1986 *Phys. Rev. Lett.* **56** 2415
Gorczyka I and Christensen N E 1991 *Solid State Commun.* **80** 335
Harrison W A 1985 *Phys. Rev.* B **31** 2121
Hedin L and Lundquist B I 1971 *J. Phys. C: Solid State Phys.* **4** 2063
Jenkins S J, Srivastava G P and Inkson J C 1994 *J. Phys. C: Solid State Phys.* **6** 8781
Lambrecht W R L and Segall B 1992 *Wide Band Gap Semiconductors* ed T D Moustakas, J I Pankove and Y Hamakawa *MRS Symp. Proc. 242* (Pittsburgh, PA: Materials Research Society) p 367
——1994 unpublished
Lei T and Moustakas T D 1992 *Wide Band Gap Semiconductors* ed T D Moustakas, J I Pankove and Y Hamakawa *MRS Symp. Proc. 242* (Pittsburgh, PA: Materials Research Society) p 433
Lei T, Moustakas T D, Graham R J, He Y and Berkowitz S J 1992 *J. Appl. Phys.* **71** 4933 and references therein
Martin G, Strite S, Thronton J and Morkoc H 1991 *Appl. Phys. Lett.* **58** 21
Methfessel M 1988 *Phys. Rev.* B **38** 1537
Min B J, Chan C T and Ho K M 1992 *Phys. Rev.* B **45** 1159
Miwa K and Fukumotoa A 1993 *Phys. Rev.* B **48** 7897
Mizuta M, Fujieda S, Matsumoto Y and Kowamura T 1986 *Japan. J. Appl. Phys.* **25** L945
Molnar R J and Moustakas T D 1993 *Bull. Am. Phys. Soc.* **38** 445
Muñoz A and Kunk K 1991 *Phys. Rev.* B **44** 10 372
Nakamura S, Senoh M and Mukai T 1991 *Japan. J. Appl. Phys.* **30** L1708
Paisley M, Sitar Z, Posthill J B and Davis R F 1989 *J. Vac. Sci. Technol.* A **7** 701
——1992 *J. Mater. Sci. Lett.* **11** 261
Perdew J P and Levy M 1983 *Phys. Rev. Lett.* **51** 1884
Perlin P, Carillon C J, Itie J P, San Miguel A I and Polian A 1992a *Phys. Rev.* B **45** 83
Perlin P, Grzegory I, Teisseyre H and Suski T 1992b *Phys. Rev.* B **45** 13 307
Perry B and Rutz R F 1978 *Appl. Phys. Lett.* **33** 319
Powell R C *et al* 1990 *Diamond, Boron Nitride, Silicon Carbide and Related Wide Bandgap Semiconductors* ed T J Glass, R F Messier and N Fujimori *MRS Symp. Proc. 162* (Pittsburgh, PA: Material Research Society) p 525
Rubio A and Cohen M L 1995 *Phys. Rev.* B **51** 4343
Rubio A, Corkill J L, Cohen M L, Shirley E L and Louie S G 1993 *Phys. Rev.* B **48** 11 810

Sanchez J M and de Fontaine D 1981 *Structure and Bonding in Crystals* vol 2, ed M O'Keefe and A Navrotsky (New York: Academic) p 117
Sanchez J M, Ducastell F and Gratias D 1984 *Physica* A **128** 334
Schrwin M E and Drummond T J 1991 *J. Appl. Phys.* **69** 8423
Sham L J and Schulter M 1983 *Phys. Rev. Lett.* **51** 1888
Srivastava G P, Martins J L and Zunger A 1985 *Phys. Rev.* B **31** 2561
Strite S, Ruan J, Li Z, Salvador A, Chen H, Smith D J, Choyke W J and Morkoc H 1991 *J. Vac. Sci. Technol.* B **9** 192
Ueno M, Yoshida M, Onodera A, Shimomura O and Takemura K 1994 *Phys. Rev.* B **41** 14
Van der Walle G 1993 *Wide Band Gap Semiconductors, Proc. 7th Semicond. Symp. (Trieste, 1993)* (Amsterdam: North-Holland) *Physica* B **185** 1–607
Wettling W and Windschif J 1984 *Solid State Commun.* **50** 33
Wyckoff R W 1964 *Crystal Structures* 2nd edn, vol 1 (New York: Wiley-Interscience)
Xia H, Xia Q and Ruof A L 1993 *Phys. Rev.* B **47** 12 925
Yeh C Y, Lu Z W, Froyen S and Zunger A 1992 *Phys. Rev.* B **46** 10 086
Yoshida S, Misawa S and Gonda S 1982 *J. Appl. Phys.* **53** 6844